Cryo-EM structures of HKU2 and SADS-CoV spike glycoproteins and insights into coronavirus evolution

Jinfang Yu[1], Shuyuan Qiao[1], Runyu Guo[1], Xinquan Wang[1,†]

[1]The Ministry of Education Key Laboratory of Protein Science, Beijing Advanced Innovation Center for Structural Biology, Beijing Frontier Research Center for Biological Structure, Collaborative Innovation Center for Biotherapy, School of Life Sciences, Tsinghua University, 100084 Beijing, China

[†]To whom correspondence should be addressed.

The authors declare no competing financial interests. Correspondence and requests for materials should be addressed to X.W. (xinquanwang@tsinghua.edu.cn).

Abstract

A new porcine coronavirus SADS-CoV was recently identified from suckling piglets with severe diarrhea in southern China and its genome sequence is most identical (~95% identity) to that of bat α-coronavirus HKU2. It again indicates bats are the natural reservoir of many coronaviruses that have great potential for cross-species transmission to animals and humans by recombination and/or mutation. Here we report the cryo-EM structures of HKU2 and SADS-CoV spike glycoprotein trimers at 2.38 Å and 2.83 Å resolution, respectively. HKU2 and SADS-CoV spikes exhibit very high structural similarity, with subtle differences mainly distributed in the NTD and CTD of the S1 subunit responsible for cell attachment and receptor binding. We systematically analyzed and compared the NTD, CTD, SD1 and SD2 domains of the S1 subunit and the S2 subunit of HKU2 spike with those of α-, β-, γ-, and δ-coronavirus spikes. The results show that the NTD and CTD of HKU2/SADS-CoV are probably the most ancestral in the evolution of spike. Although the S2 subunit mediating membrane fusion is highly conserved, the connecting region after fusion peptide in HKU2/SADS-CoV S2 subunit also adopts a conformation distinct from other coronaviruses. These results structurally demonstrate a close evolutionary relationship between HKU2 /SADS-CoV and β-coronavirus spikes and provide new insights into the evolution and cross-species transmission of coronaviruses.

Introduction

Coronaviruses, categorized into the order *Nidovirales* family *Coronaviridae* and subfamily *Coronavirinae*, are a large group of viral pathogens with a wide host range[1]. Their infections in humans, other mammals and birds can cause respiratory, hepatic, enteric and neurological diseases with varying severity[2]. The severe acute respiratory syndrome coronavirus (SARS-CoV) and Middle East respiratory syndrome coronavirus (MERS-CoV) have posed severe threats to human health in the 21st century[1,3]. In the meantime, coronaviruses infecting domestic animals also bring substantial economic losses[4]. For example, the swine acute diarrhea syndrome coronavirus (SADS-CoV) (also known as SeACoV and PEAV) isolated in 2017 caused outbreaks of severe watery diarrhea of suckling piglets with a mortality up to 90% in several commercial pig farms in Guangdong Province of China[5-10]. SADS-CoV is an α-coronavirus and other representative members in the α-genus are porcine epidemic diarrhea virus (PEDV), porcine transmissible gastroenteritis coronavirus (TGEV), porcine respiratory coronavirus (PRCV), human NL63 and 229E coronaviruses (HCoV-NL63 and HCoV-229E)[1]. Representative members in other three genera include mouse hepatitis coronavirus (MHV), bovine coronavirus (BCoV), SARS-CoV, MERS-CoV, HCoV-OC43 and HCoV-HKU1 in the β-genus, avian infectious bronchitis virus (IBV) in the γ-genus and porcine deltacoronavirus (PdCoV) in the δ-genus[1].

Cross-species transmission promoted by genetic recombination and/or mutations underlies the host range expansion of coronaviruses[3,11-13]. Bats are the natural reservoir of more than 30 different α- and β-coronaviruses that have great potential for interspecies transmission by recombination and/or mutation[12,14-16]. Data on genetic evolution, receptor binding and pathogenesis have demonstrated that human SARS-CoV and MERS-CoV most likely originate from bats[1]. Palm civets and dromedary camels are the intermediate hosts of SARS-CoV and MERS-CoV from bats to humans[1], respectively. The newly identified porcine SADS-CoV isolates are also found to share ~95% sequence identity with *Rhinolophus* bat coronavirus HKU2, and this further stressed the severe results of coronavirus spillover from bats to domestic animals[5-10].

However, the molecular mechanisms underlying the transmission of SADS-CoV from bats to pigs are still unknown and need to be further explored. Recently it was shown that SADS-CoV is able to infect cells from a broad range of species including mouse, chicken, pig, monkey and human, indicating a high potential of the SADS-CoV for interspecies transmission[17].

The spike glycoprotein of coronaviruses mediates viral entry by binding host receptor with the S1 subunit and fusing viral and cellular membranes with the S2 subunit, thereby determining viral host range and tissue tropism[18,19]. As a class I viral fusion protein, the spike exists on the envelope of virion as a homotrimer and each monomer contains more than 1000 amino acid residues that can be cleaved into S1 and S2 subunits[18]. For most coronaviruses, the N-terminal domain (NTD) of the S1 subunit (NTD) recognizes cell surface carbohydrates, while the C-terminal domain (CTD) specifically binds to cellular protein receptors[18-20]. SARS-CoV and HCoV-NL63 utilize CTD to bind human receptor ACE2[21-23]; MERS-CoV utilizes CTD to bind human receptor DPP4[24,25]; TGEV, PRCV and 229E utilize CTD to bind receptor APN[26-28]; HCoV-OC43 utilizes NTD to recognize glycans[29]; and one exception is MHV, which utilizes the NTD to bind mouse receptor CEACAM1a[30]. Therefore, the S1 subunit, especially its NTD and CTD, is the most variable region of the spike, and is responsible for different tropisms of coronaviruses. In comparison, the S2 subunit containing the fusion peptide (FP) and heptad repeats (HR1 and HR2) for membrane fusion are more conserved in both sequence and structure[18,19]. For the SADS-CoV, receptor analysis indicated that none of the known coronavirus protein receptors including ACE2, DPP4 and APN are essential for the cell entry[7,17]. There are also no reports regarding to the recognition of glycans by the NTD of SADS-CoV.

Structural studies of the spike and its binding with glycans and protein receptors have provided important insights into the origin, evolution and interspecies transmission of coronaviruses. Cryo-EM structures of spike trimer from all four coronavirus genera have been reported: the α-coronavirus spike structures are determined for HCoV-NL63[31], HCoV-229E[27] and PEDV[32]; the β-coronavirus spike structures are determined for MHV[33,34], HCoV-HKU1[35], HCoV-OC43[29], SARS-

CoV[21,36-38] and MERS-CoV[36,39,40]; the γ-coronavirus spike structure is determined for IBV[41] and the δ-coronavirus spike structure is determined for PdCoV[42,43]. The cryo-EM structures of bat coronavirus spike trimers have not been reported, and only crystal structures of the CTD from HKU4[44], HKU5[45] and HKU9[46] were determined.

The spikes of SADS-CoV (1130 amino acid residues) and HKU2 (1128 amino acid residues) are the shortest among all known coronavirus spike glycoproteins and their amino acid identities to other known coronavirus spikes are lower than 28%, indicating the spikes of HKU2 and SADS-CoV are unique[5-10,47]. In this study, we report the cryo-EM structures of the SADS-CoV and HKU2 spike trimers at 2.83 Å and 2.38 Å resolution, respectively. The HKU2 spike trimer structure is the first one from bat coronavirus. We analyzed the HKU2 and SADS-CoV trimer structures and also compared the NTD, CTD, SD1 and SD2 domains of the S1 subunit and the S2 subunit of HKU2 with other spikes from α-, β-, γ-, and δ-coronaviruses. Our results strongly support that HKU2 and SADS-CoV preserve primitive structural features in their spikes that have a close evolutionary relationship with β-coronavirus spikes and provide new insights into the evolution and cross-species transmission of coronaviruses.

Results

Protein expression and structure determination

The cDNAs encoding HKU2 spike (YP_001552236) and SADS-CoV spike (AVM41569.1) were synthesized with codons optimized for insect cell expression. HKU2 ectodomains (residues 1-1066) and SADS-CoV ectodomains (residues 1-1068) were separately cloned into pFastBac-Dual vector (Invitrogen) with C-terminal foldon tag and Strep tag. After expression in Hi5 insect cells and purification to homogeneity, the cryo-EM images on these two spike ectodomains were recorded using FEI Titan Krios microscope operating at 300 KV with a Gatan K2 Summit direct electron detector (Supplementary Fig. 1). About 1,400,000 particles for HKU2 spike and 900,000 particles for SADS-CoV spike were subjected to 2D classification, and a total of 421,490 particles of HKU2 spike and 152,334 particles of SADS-CoV spike were

selected and subjected to 3D refinement with C3 symmetry to generate density maps (Supplementary Fig. 2). The overall density maps were solved to 2.38 Å for HKU2 spike and 2.83 Å for SADS-CoV spike (gold-standard Fourier shell correlation = 0.143) (Supplementary Fig. 1 and Supplementary Fig. 2). The atomic-resolution density map enabled us to build nearly all residues of HKU2 spike ectodomains (residues 17-995) except for a few breaks (residues 129-141 and 204-204), as well as 48 N-linked glycans (Supplementary Fig. 3a and Supplementary Fig. 4a). The final refined model of SADS-CoV spike contains residues 19-998 with some short breaks (residues 134-143 and 488-490) and 45 N-linked glycans (Supplementary Fig. 3b and Supplementary Fig. 4b). Data collection and refinement statistics for these two structures are listed in Supplementary Table 1.

Overall structures of HKU2 and SADS-CoV spikes

The overall structures of HKU2 and SADS-CoV spikes we determined here resemble the previously reported pre-fusion structures of coronaviruses spikes. Both spike trimers have a mushroom-like shape (~150 Å in height and ~115 Å in width) (Fig. 1a), consisting of a cap mainly formed by β-sheets of the S1 subunit, a central stalk mainly formed by α-helices of the S2 subunit, and a root formed by twisted β-sheets and loops of the S2 subunit (Fig. 1a). In each trimer there is a C3 axis along the central stalk (Fig. 1a). The amino acid identity between HKU2 and SADS-CoV spikes is 86%, and these two spike structures are quite similar with the root mean square deviation (r.m.s.d.) being 0.53 Å for 962 aligned Cα atoms of the monomer and 0.56 Å for 2886 aligned Cα atoms of the trimer. Due to the high structural similarity, we will use the HKU2 structure to present the features of both spikes in the subsequent description, whereas significant differences between them will be pointed out only when necessary.

The S1 subunit of the HKU2 spike comprises two major domains, NTD and CTD, which are followed by two subdomains SD1 and SD2 connecting them to the S2 subunit (Fig. 1b and Fig. 1c). The S1 subunits from three monomers form the cap of the spike, in which the three CTDs in the inner part are at the apex sitting on top of the central stalk and the three NTDs are located outside the CTDs surrounding the central stalk

(Fig. 1a). The NTD, CTD, SD1 and SD2 of the S1 subunit are all mainly composed of β strands regarding to the secondary structure feature (Fig. 1c). In contrast, the upstream helix (UH), fusion peptide (FP), connecting region (CR), heptad repeat 1 (HR1) and central helix (CH) of the S2 subunit are mainly composed of helices, whereas the β-hairpin (BH) and subdomain 3 (SD3) at the bottom part of the S2 subunit mainly consist of β stands and loops (Fig. 1c). Moreover, the residues after the SD3, which contain the heptad repeat 2 (HR2), are not resolved in the HKU2 and SADS-CoV spike structures, as well as in all other reported coronavirus spike structures in the pre-fusion state.

The SD1 and SD2 of the S1 subunit and the S2 subunit are highly similar in amino acid sequence (85%, 84% and 95% identities) and structure (Cα r.m.s.d. less than 0.5 Å) between HKU2 and SADS-CoV spikes (Supplementary Fig. 5). The NTD has the lowest sequence identity of 70% among all domains. Structural superimposition also gave a Cα r.m.s.d. of 1.2 Å between these two NTDs, and conformational variations reside in the loops, although the core β sheet structure is structurally conserved (Supplementary Fig. 5a). The CTD sequence identity between HKU2 and SADS-CoV spikes is 82%, but the Cα r.m.s.d. between these two CTDs is 1.1 Å, also indicating structural variations in the CTD in comparison with the highly conserved SD1, SD2 and S2 subunit. The NTD and CTD of the S1 subunit are commonly utilized by coronaviruses for binding cell-surface carbohydrates or protein receptors for cell attachment[20]. Therefore, the sequence and/or structural variations indicate that HKU2 and SADS-CoV would also bind different host receptors by NTD and/or CTD of the S1 subunit, although their receptors in bat and pig are unknown and the receptor-binding sites on spike have not been defined.

NTD structure and comparisons

The NTD of HKU2 has three layers of antiparallel β-sheet with the top one consisting of six strands, the middle one consisting of five strands and the bottom one consisting of three strands. Below the bottom sheet is a short α-helix (Fig. 2a). The top and middle β-sheets form a galectin-like β-sandwich fold, which is inserted between two stands of the bottom sheet (Fig. 2a). To supplement, three disulfide bonds are detected in the

HKU2 NTD structure: C^{17}-C^{56} connecting the N-terminus of the NTD to its upper loop, C^{124}-C^{149} connecting β6 and β7 stands in the top sheet and C^{234}-C^{244} connecting the bottom helix to the bottom sheet (Fig. 2a).

Although the NTDs of all coronaviruses adopt a similar overall architecture, the NTD of HKU2 has the highest structural similarity with the NTD1 (named domain 0 in previous reports) of α-coronavirus HCoV-NL63 with an r.m.s.d. of 2.7 Å for 186 aligned Cα atoms (Fig. 2b and Supplementary Fig. 7d). The NTD1 of α-coronavirus PEDV is not completely modeled in the spike trimer structure, however the partial model still fits well with the NTD of HKU2 with an r.m.s.d. of 2.3 Å for 73 aligned Cα atoms. Both HCoV-NL63 and PEDV have a second NTD (NTD2, also named domain A in previous reports), and the NTD of HKU2 is structurally less similar to the NTD2 with an r.m.s.d. of 4.3 Å against HCoV-NL63 NTD2 and of 4.1 Å against PEDV NTD2 (Fig. 2b and Supplementary Fig. 7d). Recent structural determination showed that another α-coronavirus, HCoV-229E, also has one NTD, which is more structurally similar to the NTD2 (Cα r.m.s.d. of 2.0 Å) than the NTD1 (Cα r.m.s.d. of 3.7 Å) of HCoV-NL63 (Fig. 2b). All above comparisons indicate that there are two subtypes of NTD in the α-coronaviruses: the subtype I represented by the NTDs of HKU2 and SADS-CoV and the NTD1s of HCoV-NL63 and PEDV, and the subtype II represented by the NTD of HCoV-229E and the NTD2s of HCoV-NL63 and PEDV (Fig. 2b). Although sharing an overall architecture, these two NTD subtypes have a structural difference in the galectin-like β-sandwich fold containing the top and middle sheets stacked together through hydrophobic interactions. These two β sheets are well aligned in the galectin-like domain of subtype I, whereas there is an alignment shift in the galectin-like domain of subtype II (Fig. 2b). The other notable difference is the distribution of signature disulfide bonds. A signature disulfide bond C^{124}-C^{149} (numbered in HKU2 and connecting β6 and β7 stands in the top sheet) is conserved in all subtype I NTDs (Fig. 2b), and the subtype II NTDs have two signature disulfide bonds: the first one C^{145}-C^{168} (numbered in HCoV-229E) connecting β5 and β6 strands and the second one C^{81}-C^{105} (numbered in HCoV-229E) connecting β2 and neighbor

loop (Fig. 2b). Besides, C^{234}-C^{244} (numbered in HKU2 and connecting the bottom helix to the bottom sheet) is conserved in both subtype I and subtype II NTDs (Fig. 2b).

The NTDs of β-coronaviruses including BCoV, HCoV-HKU1, HCoV-OC43, MERS-CoV, SARS-CoV and MHV resemble the subtype I, rather than the subtype II NTD in the topology and distribution of the disulfide bonds (Fig. 2c). These β-coronavirus NTDs have additional loops in the N-terminus, between β1 and β2 strands, and between β6 and β7 stands (numbered in HKU2 structure), forming an extensive ceiling-like structure on top of the galectin-like fold (Fig. 2c). It has been found that the evolvement of this ceiling-like structure has functional outcomes such as immune evasion or receptor binding[41]. The NTD of γ-coronavirus IBV also resemble the subtype I NTD in the topology, although its disulfide bond positions are not conserved as in the subtype I NTD (Fig. 2d). To be note, the NTD of δ-coronavirus PdCoV resemble the subtype II NTD in the topology and distribution of the disulfide bonds (Fig. 2e). Both IBV and PdCoV NTDs also have additional insertions including loops and short helices in the galectin-like fold compared to the two subtypes of NTD in α-coronaviruses (Fig. 2d and Fig. 2e).

CTD structure and comparisons

The CTD of HKU2 has a twisted five-stranded antiparallel β sheet as the core with connecting loops between the stands (Fig. 3a). It contains four disulfide bonds: C^{277}-C^{300} and C^{285}-C^{290} at the N-terminus, C^{341}-C^{397} at the C-terminus and the last one C^{331}-C^{369} connecting the β2 and β5 strands in the core β sheet (Fig. 3a). Interestingly, the CTD core of HKU2 is of high structural similarity with the conserved CTD core of β-coronaviruses and the disulfide bonds in the CTD of HKU2 except for C^{285}-C^{290} are also detected in all β-coronavirus CTDs (Fig. 3b). These CTDs have the core of one twisted β-sheet and here we name them as one-layer CTD subtype (Fig. 3a and Fig. 3b). The β-coronavirus CTDs always have an insertion consisting of loops and/or stands between the β5 and β6 strands of the core (Fig. 3b). SARS-CoV, MERS-CoV, HKU4 and HKU5 have receptor-binding motif (RBM) in this insertion region responsible for

binding their respective protein receptors[45]. In the CTD of HKU2, there is only one short loop between the β5 and β6 strands of the core twisted β-sheet (Fig. 3a).

Although as members in the α-genus, HKU2 and SADS-CoV CTD structures are significantly different from those of other α-coronaviruses HCoV-NL63, HCoV-229E, PEDV, TGEV and PRCV that contain two layers of β-sheets (Fig. 3c). And we named these CTDs as two-layer CTD subtype. All available two-layer CTD structures can be well aligned with Cα r.m.s.d. in the range of 1.0-3.4 Å, except for the CTDs of HKU2 and SADS-CoV. These two-layer CTDs contain two highly conserved disulfide bonds: C^{540}-C^{586} and C^{569}-C^{596} (numbered in PEDV CTD) (Fig. 3c). The C^{569}-C^{596} is conserved among all coronaviruses, whereas the C^{540}-C^{586} is conserved in all α-coronaviruses (except for HKU2 and SADS) and δ-coronavirus PdCoV (Fig. 3c).

The CTD of δ-coronavirus PdCoV have a core of two β-sheets, belonging to the two-layer CTD subtype (Fig. 3c). As for the γ-coronavirus IBV, the core of its CTD is also similar to the typical two-layer CTD (Fig. 3c). However, several β strands are replaced by loops and the disulfide bonds are in different positions from the two-layer CTD (Fig. 3c). IBV CTD also has an extra region of loops, reminiscent of the extra domain in the CTDs of β-coronaviruses (Fig. 3c).

SD1 and SD2 structures and comparisons

The SD1 and SD2 are two subdomains following the CTD in the S1 subunit, linking the CTD to the S2 subunit. The HKU2 SD1 is a partial β barrel consisting of five β strands and a disulfide bond (C^{409}-C^{458}) connecting its C-terminus to the β1 strand (Fig. 4a). This five-stranded β barrel and the linking disulfide bond are conserved among all four genera of coronavirus (Fig. 4a). The HKU2 SD2 has a structure of two layers of β-sheet with an additional short α-helix over the top sheet (Fig. 4b). The additional α-helix and the top sheet is linked by a disulfide bond (C^{482}-C^{509}), and another disulfide bond (C^{524}-C^{533}) links the C-terminal loop to the bottom sheet (Fig. 4b). The two-layer core structure and the second disulfide bond are conserved among all genera of coronavirus, however, the additional α helix and the first linking disulfide bond is a

distinct feature of β-coronaviruses plus α-coronavirus HKU2 and SADS-CoV (Fig. 4b). This additional helix appears to be an insertion between the primitive β2 and β3 strands of the SD2, and is retained during evolution of β-coronaviruses.

Quaternary packing of the NTD and CTD in the spike

It has been observed that coronaviruses have two types of quaternary packing mode of the S1 subunits in the trimer: intra-subunit packing and cross-subunit packing[41]. Actually, this is mainly caused by different positioning and interaction between NTD and CTD in the spike monomer. The HKU2 S1 subunit, similar to those in α-coronaviruses HCoV-NL63, HCoV-226E and PEDV and δ-coronavirus PdCoV, have an "inward" CTD which contacts with the NTD (Fig. 5a). The three structural "NTD-CTD" modules in the cap region of these spikes are composed of NTD and CTD from the same monomer, forming the intra-subunit packing in the spike trimer (Fig. 5a). The S1 subunits of other coronaviruses in the β- and γ-genera including MHV, SARS-CoV, MERS-CoV, HCoV-OC43 and IBV have an "outward" CTD that is far away from the NTD (Fig. 5b). Therefore, the three structural "NTD-CTD" modules in the cap region of these spikes have the NTD from one monomer and the CTD from the adjacent monomer, forming the cross-subunit packing in the spike trimer (Fig. 5b). Interestingly, we found that the "outward" CTDs always have an insertion in the core structure, such as β-coronavirus CTDs and γ-coronavirus IBV CTD (Fig. 5b). In contrast, all "inward" CTDs only have the one-layer or two-layer core structure without obvious inserted region.

Conserved S2 subunit and a distinct CR

Sequence analysis suggested that the S1/S2 protease cleavage site at the boundary between the S1 and S2 subunits is R544-M545 in HKU2 spike and R546-M547 in SADS-CoV spike[5,8,47]. Compared to the S1 subunit, the topology and structure of S2 subunit are highly conserved in all coronavirus spikes. The HKU2 S2 subunit contains a 3-helix upstream helix (UH) (residues 589-639), a fusion peptide helix (FP) (residues 672-684), a connecting region (CR) (residues 689-747), a 4-helix heptad repeat 1 (HR1)

(residues 748-836), a central helix (CH) (residues 837-887), a twisted β-hairpin (BH) (residues 888-929) and a β-sandwich like SD3 (residues 930-995) (Fig. 1b and Fig. 6a). Like in other coronavirus spikes in the prefusion state, the model of HR2 after SD3 was not built in the structure due to poor density. Five disulfide bonds in S2 are detected. Two of them (C^{590}-C^{612} and C^{595}-C^{601}) stabilize the folded helices of UH, C^{696}-C^{706} bends the CR, C^{884}-C^{895} links the CH and the BH, and C^{934}-C^{943} is within the SD3 (Fig. 6a). The first four disulfide bonds are conserved in all coronaviruses, and the last one in the SD3 has different positions in different spikes. Specifically, it links the β2 and β3 stands of SD3 in the spikes of HKU2, SADS-CoV and MERS-CoV (numbered in MERS-CoV), and in other coronavirus spikes it links the β2 stand to the C-terminal loop of SD3 (numbered in MERS-CoV) (Supplementary Fig. 6).

All coronavirus spikes have the S2' protease site upstream from the FP in the S2 subunit, which is essential for proteolytic fusion activation of the spike. Receptor binding and cleavage at the S2' site promote large-scale conformational changes of the FP, CR, HR1 and HR2, allowing the insertion of FP into host cell membrane and the formation of six-helix bundle. The FP and CR, which are often not well and totally resolved in other coronavirus spike structures, can be clearly modeled in the HKU2 spike due to the atomic resolution of the map (Supplementary Fig. 4). The typical CR in the S2 subunit contains three helices and one short strand, with a disulfide bond bending the first and second helix to form a turning (Fig. 6b). In HKU2, the second helix is replaced by a short strand (713-716) and the third helix is replaced by a loop (721-741), therefore there are two short strands and only one helix in HKU2 CR (Fig. 6c). The conserved disulfide bond C^{696}-C^{706} makes the first helix of CR in HKU2 spike turn upside down. The S2' cleavage site (between R671 and S672) is then covered by the reversed CR helix and loops, and R671 interacts with E723 in the loop and K697 and K698 in helix 1 (Fig. 6c). In other coronaviruses, taking the MHV S2 for example, the helix 1 does not cover the S2' site (between R869 and S870), and R869 only loosely interacts with T929 in helix 3 (Fig. 6b). After the dissociation of the S1 subunit triggered by receptor binding, the exposure of the S2' site for cleavage is a prerequisite for the proteolytic activation of the coronavirus spike to mediate membrane fusion. The buried

S2' site indicates that HKU2 spike, compared to other coronavirus spikes, would require more conformational changes around the S2' site for the exposure.

Discussion

A new porcine coronavirus SADS-CoV (also named as SeACoV and PEAV in other reports) was recently identified from suckling piglets with diarrhea in southern China, and its genome sequence was most identical (~95% identity) to that of *Rhinolophus* bat α-coronavirus HKU2[5-10]. The SADS-CoV and HKU2 are phylogenetically located in a sub-lineage closely related to the proposed α-coronavirus group-1b lineage at the complete genome level[5-10]. However, phylogenetic analysis based on the spike glycoprotein indicated that they are members of a separate lineage clustered within β-coronavirus (Supplementary Fig. 7a), suggesting that HKU2 and SADS-CoV probably resulted from recombination of an α-coronavirus with an unrecognized β-coronavirus S gene[5-10]. These results, together with the lower than 28% amino acid identities to other known coronavirus glycoproteins, strongly indicate that the spike glycoproteins of HKU2 and SADS-CoV are unique[5-10]. In this study, we determined the cryo-EM structures of HKU2 and SADS-CoV spike glycoproteins at atomic resolutions. Pairwise comparisons demonstrated nearly identical overall structures, and differences mainly locate in the loops of NTD and CTD of the S1 subunit between the spikes of HKU2 and SADS-CoV (Supplementary Fig. 5). A series of structural analysis and comparisons were also performed at the domain level between HKU2 spike with other coronavirus spikes with determined structures. Our results show that HKU2 and SADS-CoV spikes maintain primitive structural features, especially in the NTD and CTD, and provide more insights into the evolution of coronaviruses.

The HKU2 and SADS-CoV have one NTD in the S1 subunit, and their structures are more similar to the NTD1 than the NTD2 of α-coronaviruses HCoV-NL63 and PEDV, whereas the only NTD of HCoV-229E is structurally more similar to the NTD2 than the NTD1 (Fig. 2). Therefore, we suggest that α-coronaviruses have two subtypes of NTD. The evolution relationship between them are not clear yet. It was once

363 suggested that the presence of two NTDs in HCoV-NL63 is a result of gene
364 duplication[31]. However, the sequence identity between these two NTDs is only 15.7%
365 in HCoV-NL63 and 12.9% in PEDV. Considering that HKU2 (SADS-CoV) and
366 HCoV-229E have one NTD belonging to either subtype I or subtype II, a more plausible
367 evolution way of the NTD in α-coronaviruses is the recombination of two separate
368 primitive domains into the genome, resulting in the presence of two NTDs in the S1
369 subunit α-coronaviruses including HCoV-NL63 and PEDV. To be note, these two NTD
370 subtypes may represent primitive structures that could be the evolutionary ancestors of
371 NTDs of other genera coronaviruses. For example, in the current available spike
372 structures, the NTDs of β-coronavirus are similar to the HKU2 NTD representing the
373 subtype I in both architecture and disulfide bond positions. These β-coronavirus NTDs
374 also have additional loop ceiling over the top sheet, functionally facilitating immune
375 evasion or binding protein receptor such as in MHV[30]. The NTD of γ-coronavirus IBV
376 is also architecturally similar to the subtype I, although the disulfide bond positions are
377 not conserved (Fig. 2d). In contrast, the δ-coronavirus PdCoV NTD is similar to the
378 HCoV-229E NTD representing the subtype II in both architecture and disulfide bond
379 positions (Fig. 2e). A previous study of the IBV spike proposed that α-coronavirus
380 NTDs are probably the most ancestral and the NTDs of the four genera form an
381 evolutionary spectrum in the order of α-, δ-, γ-, and β-genus[41]. Our proposal here is
382 similar to the previous one in the point that two NTD subtypes in α-coronaviruses may
383 represent primitive structures that could be the evolutionary ancestors of NTDs.
384 However, we argue that the evolution pathways may not be in the order of α-, δ-, γ-,
385 and β-genus. A more plausible pathway is that the β-, γ- and δ-coronavirus NTDs may
386 evolve independently and parallelly from subtype I (β- and γ-coronavirus NTDs) or
387 subtype II (δ-coronavirus NTDs) (Supplementary Fig. 7b).

388 The HKU2 and SADS-CoV CTD structure have a one-layer core consisting of a
389 twisted five-stranded antiparallel β sheet. Interestingly, β-coronavirus CTDs also have
390 the similar one-layer core structure and three strictly conserved disulfide bonds are also
391 present in the core of HKU2 CTD. Currently, all identified receptor-binding motif of β-
392 coronavirus CTDs are within an inserted domain between two stands of the core sheet,

and this insertion responsible for receptor binding of β-coronaviruses is replaced by a short loop in HKU2 CTD. This result firstly indicates HKU2 CTD represent a primitive structure in the one-layer CTD family, while the inserted domain in β-coronaviruses results from a recombinant event during evolution (Supplementary Fig. 7c). The second indication is that HKU2 and SADS-CoV may not utilize the CTD to bind protein receptors that have not been identified yet, and their different receptor usage may be determined by the NTD that harbors almost 50% of residue difference between them. To be note, the CTDs from other α-coronaviruses, γ-coronavirus IBV and δ-coronavirus PdCoV all belong to the two-layer subtype consisting of two layers β-sheets, although with structural variations in different viruses. These results further confirmed the previous phylogenetic analysis suggesting that HKU2 and SADS-CoV probably resulted from a recombination of an α-coronavirus genomic backbone with an unrecognized β-coronavirus spike gene[5,8,47].

In contrast with the NTD and CTD having unique structural feathers, the SD1 and SD2 domains of the S1 subunit and the S2 subunits of HKU2 and SADS-CoV are structurally conserved as those of other coronaviruses. In the evolutionary aspect, it is not surprising because this region either connects the CTD to the S2 subunit (SD1 and SD2) or mediates the membrane fusion, whereas the NTD and CTD are key factors determining tissue tropism and host range of coronaviruses[20]. Even highly conserved in overall structure, the S2 subunit in HKU2 and SADS-CoV still have a secondary structure arrangement in the connecting region (CR) after the fusion peptide (FP), resulting in a more buried S2' cleavage site (Fig. 6c). It indicates that although the membrane fusion mechanism is highly conserved, the dynamic fusion procedures of HKU2 and SADS-CoV may still have their unique features that need to be addressed in the future.

Since the outbreak of SARS epidemic in 2002-2003, new coronaviruses including MERS-CoV, HCoV-HKU1, HCoV-NL63 in human and PdCoV and SADS-CoV in livestock has been identified[1,16]. Extensive studies also revealed a diversity of coronaviruses in bats that could be the source for emergence of zoonotic epidemics such as SARS in the past and new one in the future[1,12,16]. The spikes of bat coronavirus

HKU2 and porcine coronavirus SADS-CoV (1128 and 1130 residues) are the shortest among all current known coronavirus spike glycoproteins and their NTDs and CTDs may also represent evolutionary ancestors[5-9,47]. In comparing the structures of HKU2 and SADS-CoV spikes with other coronavirus spikes, we observed that additional NTDs could be recombined, ceiling loops could be inserted into NTD core, and extra domain containing receptor-binding motif could be inserted into the CTD core structure. These phenomena indicate the subdomains are gradually recruited into the S1 subunit during evolution, and the recruitments are required for cross-species transmission, adapting to different host range, and responding to the updating of host immune system, which provides a vivid example for the co-evolution of virus and host.

Acknowledgements

We thank the Tsinghua University Branch of China National Center for Protein Sciences (Beijing) for providing the facility support. This work was supported by funds from Beijing Advanced Innovation Center for Structural Biology at Tsinghua University and the National Key Plan for Scientific Research and Development of China (grant number 2016YFD0500307).

Author contributions

J.Y. carried out protein expression, purification, electron microscopy sample preparation, data collection, image processing and model building with the help of S.Q. X.W. conceived, designed and directed the study. X.W., J.Y. and R.G analyzed the structure, made the figures and wrote the manuscript.

References

1 Cui, J., Li, F. & Shi, Z. L. Origin and evolution of pathogenic coronaviruses. *Nat Rev Microbiol* **17**, 181-192, doi:10.1038/s41579-018-0118-9 (2019).

2 Fehr, A. R. & Perlman, S. Coronaviruses: an overview of their replication and pathogenesis. *Methods Mol Biol* **1282**, 1-23, doi:10.1007/978-1-4939-2438-7_1 (2015).

3 Su, S. *et al.* Epidemiology, Genetic Recombination, and Pathogenesis of Coronaviruses. *Trends*

Microbiol **24**, 490-502, doi:10.1016/j.tim.2016.03.003 (2016).

4 Wang, Q., Vlasova, A. N., Kenney, S. P. & Saif, L. J. Emerging and re-emerging coronaviruses in pigs. *Curr Opin Virol* **34**, 39-49, doi:10.1016/j.coviro.2018.12.001 (2019).

5 Fu, X. *et al.* Newly emerged porcine enteric alphacoronavirus in southern China: Identification, origin and evolutionary history analysis. *Infect Genet Evol* **62**, 179-187, doi:10.1016/j.meegid.2018.04.031 (2018).

6 Xu, Z. *et al.* Isolation and characterization of a highly pathogenic strain of Porcine enteric alphacoronavirus causing watery diarrhoea and high mortality in newborn piglets. *Transbound Emerg Dis* **66**, 119-130, doi:10.1111/tbed.12992 (2019).

7 Zhou, P. *et al.* Fatal swine acute diarrhoea syndrome caused by an HKU2-related coronavirus of bat origin. *Nature* **556**, 255-258, doi:10.1038/s41586-018-0010-9 (2018).

8 Pan, Y. *et al.* Discovery of a novel swine enteric alphacoronavirus (SeACoV) in southern China. *Vet Microbiol* **211**, 15-21, doi:10.1016/j.vetmic.2017.09.020 (2017).

9 Gong, L. *et al.* A New Bat-HKU2-like Coronavirus in Swine, China, 2017. *Emerg Infect Dis* **23**, doi:10.3201/eid2309.170915 (2017).

10 Wang, L., Su, S., Bi, Y., Wong, G. & Gao, G. F. Bat-Origin Coronaviruses Expand Their Host Range to Pigs. *Trends Microbiol* **26**, 466-470, doi:10.1016/j.tim.2018.03.001 (2018).

11 Parrish, C. R. *et al.* Cross-species virus transmission and the emergence of new epidemic diseases. *Microbiol Mol Biol Rev* **72**, 457-470, doi:10.1128/MMBR.00004-08 (2008).

12 Lu, G., Wang, Q. & Gao, G. F. Bat-to-human: spike features determining 'host jump' of coronaviruses SARS-CoV, MERS-CoV, and beyond. *Trends Microbiol* **23**, 468-478, doi:10.1016/j.tim.2015.06.003 (2015).

13 Peck, K. M., Burch, C. L., Heise, M. T. & Baric, R. S. Coronavirus Host Range Expansion and Middle East Respiratory Syndrome Coronavirus Emergence: Biochemical Mechanisms and Evolutionary Perspectives. *Annu Rev Virol* **2**, 95-117, doi:10.1146/annurev-virology-100114-055029 (2015).

14 Woo, P. C., Lau, S. K., Huang, Y. & Yuen, K. Y. Coronavirus diversity, phylogeny and interspecies jumping. *Exp Biol Med (Maywood)* **234**, 1117-1127, doi:10.3181/0903-MR-94 (2009).

15 Woo, P. C. *et al.* Discovery of seven novel Mammalian and avian coronaviruses in the genus deltacoronavirus supports bat coronaviruses as the gene source of alphacoronavirus and betacoronavirus and avian coronaviruses as the gene source of gammacoronavirus and deltacoronavirus. *J Virol* **86**, 3995-4008, doi:10.1128/JVI.06540-11 (2012).

16 Fan, Y., Zhao, K., Shi, Z. L. & Zhou, P. Bat Coronaviruses in China. *Viruses* **11**, doi:10.3390/v11030210 (2019).

17 Yang, Y. L. *et al.* Broad Cross-Species Infection of Cultured Cells by Bat HKU2-Related Swine Acute Diarrhea Syndrome Coronavirus and Identification of Its Replication in Murine Dendritic Cells In Vivo Highlight Its Potential for Diverse Interspecies Transmission. *J Virol* **93**, doi:10.1128/JVI.01448-19 (2019).

18 Li, F. Structure, Function, and Evolution of Coronavirus Spike Proteins. *Annu Rev Virol* **3**, 237-261, doi:10.1146/annurev-virology-110615-042301 (2016).

19 Tortorici, M. A. & Veesler, D. Structural insights into coronavirus entry. *Adv Virus Res* **105**, 93-116, doi:10.1016/bs.aivir.2019.08.002 (2019).

20 Li, F. Receptor recognition mechanisms of coronaviruses: a decade of structural studies. *J Virol* **89**, 1954-1964, doi:10.1128/JVI.02615-14 (2015).

21 Song, W., Gui, M., Wang, X. & Xiang, Y. Cryo-EM structure of the SARS coronavirus spike glycoprotein in complex with its host cell receptor ACE2. *PLoS Pathog* **14**, e1007236, doi:10.1371/journal.ppat.1007236 (2018).

22 Wu, K., Li, W., Peng, G. & Li, F. Crystal structure of NL63 respiratory coronavirus receptor-binding domain complexed with its human receptor. *Proc Natl Acad Sci U S A* **106**, 19970-19974, doi:10.1073/pnas.0908837106 (2009).

23 Li, F., Li, W., Farzan, M. & Harrison, S. C. Structure of SARS coronavirus spike receptor-binding domain complexed with receptor. *Science* **309**, 1864-1868, doi:10.1126/science.1116480 (2005).

24 Wang, N. *et al.* Structure of MERS-CoV spike receptor-binding domain complexed with human receptor DPP4. *Cell Res* **23**, 986-993, doi:10.1038/cr.2013.92 (2013).

25 Lu, G. *et al.* Molecular basis of binding between novel human coronavirus MERS-CoV and its receptor CD26. *Nature* **500**, 227-231, doi:10.1038/nature12328 (2013).

26 Reguera, J. *et al.* Structural bases of coronavirus attachment to host aminopeptidase N and its inhibition by neutralizing antibodies. *PLoS Pathog* **8**, e1002859, doi:10.1371/journal.ppat.1002859 (2012).

27 Li, Z. *et al.* The human coronavirus HCoV-229E S-protein structure and receptor binding. *Elife* **8**, doi:10.7554/eLife.51230 (2019).

28 Wong, A. H. M. *et al.* Receptor-binding loops in alphacoronavirus adaptation and evolution. *Nat Commun* **8**, 1735, doi:10.1038/s41467-017-01706-x (2017).

29 Tortorici, M. A. *et al.* Structural basis for human coronavirus attachment to sialic acid receptors. *Nat Struct Mol Biol* **26**, 481-489, doi:10.1038/s41594-019-0233-y (2019).

30 Peng, G. *et al.* Crystal structure of mouse coronavirus receptor-binding domain complexed with its murine receptor. *Proc Natl Acad Sci U S A* **108**, 10696-10701, doi:10.1073/pnas.1104306108 (2011).

31 Walls, A. C. *et al.* Glycan shield and epitope masking of a coronavirus spike protein observed by cryo-electron microscopy. *Nat Struct Mol Biol* **23**, 899-905, doi:10.1038/nsmb.3293 (2016).

32 Wrapp, D. & McLellan, J. S. The 3.1-Angstrom Cryo-electron Microscopy Structure of the Porcine Epidemic Diarrhea Virus Spike Protein in the Prefusion Conformation. *J Virol* **93**, doi:10.1128/JVI.00923-19 (2019).

33 Walls, A. C. *et al.* Cryo-electron microscopy structure of a coronavirus spike glycoprotein trimer. *Nature* **531**, 114-117, doi:10.1038/nature16988 (2016).

34 Walls, A. C. *et al.* Tectonic conformational changes of a coronavirus spike glycoprotein promote membrane fusion. *Proc Natl Acad Sci U S A* **114**, 11157-11162, doi:10.1073/pnas.1708727114 (2017).

35 Kirchdoerfer, R. N. *et al.* Pre-fusion structure of a human coronavirus spike protein. *Nature* **531**, 118-121, doi:10.1038/nature17200 (2016).

36 Yuan, Y. *et al.* Cryo-EM structures of MERS-CoV and SARS-CoV spike glycoproteins reveal the dynamic receptor binding domains. *Nat Commun* **8**, 15092, doi:10.1038/ncomms15092 (2017).

37 Gui, M. *et al.* Cryo-electron microscopy structures of the SARS-CoV spike glycoprotein reveal a prerequisite conformational state for receptor binding. *Cell Res* **27**, 119-129, doi:10.1038/cr.2016.152 (2017).

38 Kirchdoerfer, R. N. *et al.* Stabilized coronavirus spikes are resistant to conformational changes induced by receptor recognition or proteolysis. *Sci Rep* **8**, 15701, doi:10.1038/s41598-018-

34171-7 (2018).

39 Pallesen, J. *et al.* Immunogenicity and structures of a rationally designed prefusion MERS-CoV spike antigen. *Proc Natl Acad Sci U S A* **114**, E7348-E7357, doi:10.1073/pnas.1707304114 (2017).

40 Park, Y. J. *et al.* Structures of MERS-CoV spike glycoprotein in complex with sialoside attachment receptors. *Nat Struct Mol Biol* **26**, 1151-1157, doi:10.1038/s41594-019-0334-7 (2019).

41 Shang, J. *et al.* Cryo-EM structure of infectious bronchitis coronavirus spike protein reveals structural and functional evolution of coronavirus spike proteins. *PLoS Pathog* **14**, e1007009, doi:10.1371/journal.ppat.1007009 (2018).

42 Shang, J. *et al.* Cryo-Electron Microscopy Structure of Porcine Deltacoronavirus Spike Protein in the Prefusion State. *J Virol* **92**, doi:10.1128/JVI.01556-17 (2018).

43 Xiong, X. *et al.* Glycan Shield and Fusion Activation of a Deltacoronavirus Spike Glycoprotein Fine-Tuned for Enteric Infections. *J Virol* **92**, doi:10.1128/JVI.01628-17 (2018).

44 Wang, Q. *et al.* Bat origins of MERS-CoV supported by bat coronavirus HKU4 usage of human receptor CD26. *Cell Host Microbe* **16**, 328-337, doi:10.1016/j.chom.2014.08.009 (2014).

45 Han, X. *et al.* Structure of the S1 subunit C-terminal domain from bat-derived coronavirus HKU5 spike protein. *Virology* **507**, 101-109, doi:10.1016/j.virol.2017.04.016 (2017).

46 Huang, C. *et al.* Putative Receptor Binding Domain of Bat-Derived Coronavirus HKU9 Spike Protein: Evolution of Betacoronavirus Receptor Binding Motifs. *Biochemistry* **55**, 5977-5988, doi:10.1021/acs.biochem.6b00790 (2016).

47 Lau, S. K. *et al.* Complete genome sequence of bat coronavirus HKU2 from Chinese horseshoe bats revealed a much smaller spike gene with a different evolutionary lineage from the rest of the genome. *Virology* **367**, 428-439, doi:10.1016/j.virol.2007.06.009 (2007).

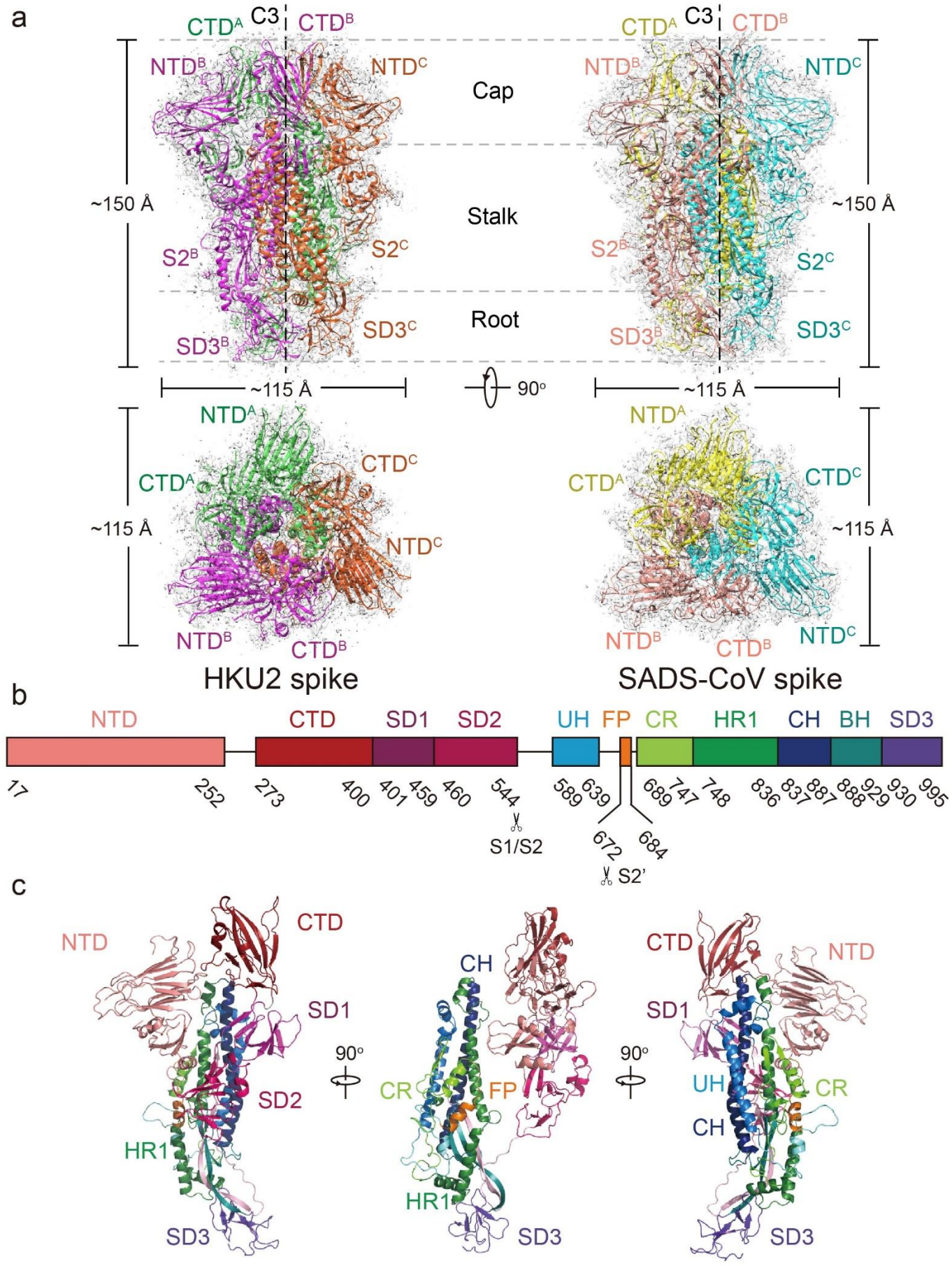

Fig. 1 Overall structures of HKU2 and SADS-CoV spike glycoproteins. (a) Overall structures of HKU2 and SADS-CoV spike glycoproteins shown in side view (upper panel) and top view (lower panel). Three monomers of HKU2 spike are colored magenta, green, and orange, respectively; three monomers of SADS-CoV spike are colored pink, yellow, and cyan, respectively. The cryo-EM maps are shown as semitransparent surface and contoured at 2.6 RMS and 3 RMS for HKU2 and

SADS-CoV spikes, respectively. The trigonal axes are shown as black dashed lines. Visible segments of each monomer are labeled accordingly. The cap, stalk and root parts are partitioned by gray dashed lines. **(b)** Segmentation of HKU2 monomer. The segments of HKU2 are shown as boxes with the width related to the length of amino acid sequence. The start and end amino acids of each segment are labeled. The position of S1/S2, and S2' cleavage sites are indicated. NTD, N-terminal domain; CTD, C-terminal domain; SD1, subdomain 1; SD2, subdomain 2; UH, upstream helix; FP, fusion peptide; CR, connecting region; HR1, heptad repeat 1; CH, central helix; BH, β-hairpin; SD3, subdomain 3. **(c)** Overall structure of HKU2 monomer. Side views of HKU2 monomer shown in three directions. The segments are colored the same as in b.

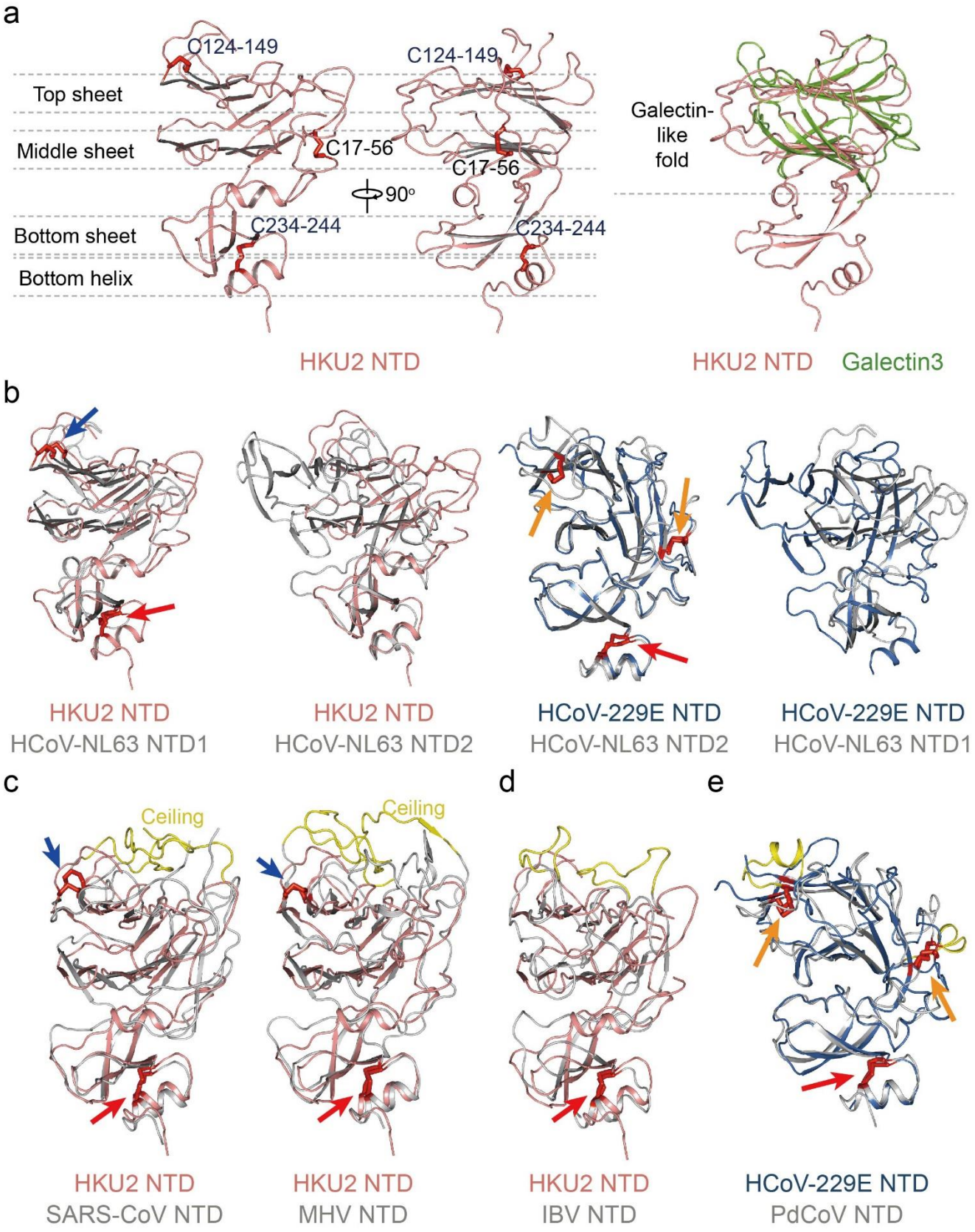

Fig. 2 Structure of HKU2 NTD and comparisons. (a) Structure of HKU2 NTD. Side views of HKU2 NTD are shown in two orthogonal directions. Disulfide bonds are shown as red sticks. Conserved disulfide bonds are labeled blue; other disulfide bonds are labeled black. Top sheet, middle sheet, bottom sheet, and bottom helix are partitioned by gray dashed lines. Comparison of HKU2 NTD and galectin3 are shown in the right panel. HKU2 NTD is colored salmon; galectin3 is colored green. PDB code: galectin3, 1A3K. **(b)** Two subtypes of α-coronavirus NTD. Structural alignments of HKU2 NTD with HCoV-NL63 NTD1, and with HCoV-NL63 NTD2 are shown in the left two panels; structural alignments of HCoV-229E NTD with HCoV-NL63 NTD1, and with HCoV-NL63 NTD2 are shown in the right two panels. HKU2 NTD is colored salmon;

HCoV-229E NTD is colored marine; HCoV-NL63 NTD1 and NTD2 are colored gray. Disulfide bonds are shown as red sticks. Disulfide bonds conserved in both types of NTDs are indicated by red arrows; disulfide bonds conserved in subtype I NTD are indicated by blue arrows; disulfide bonds conserved in subtype II NTD are indicated by orange arrows. PDB codes: HCoV-229E, 6U7H; HCoV-NL63, 5SZS. **(c)** β-coronavirus NTDs resemble subtype I. Structural alignments of HKU2 NTD with SARS-CoV NTD, and with MHV NTD are shown. Disulfide bonds are shown and labeled the same as in b. Ceilings in β-coronavirus NTDs are shown in yellow. PDB codes: SARS, 5XLR; MHV, 3JCL. **(d)** γ-coronavirus IBV NTD resembles subtype I. Structural alignment of HKU2 NTD with IBV NTD is shown. Disulfide bonds are shown and labeled the same as in b. The additional loops in IBV NTD is shown in yellow. PDB code: IBV, 6CV0. **(e)** δ-coronavirus PdCoV NTD resembles subtype II. Structural alignment of HCoV-229E NTD with PdCoV NTD is shown. Disulfide bonds are shown and labeled the same as in b. The additional helices in PdCoV NTD are shown in yellow. PDB codes: HCoV-229E, 6U7H; PdCoV, 6B7N.

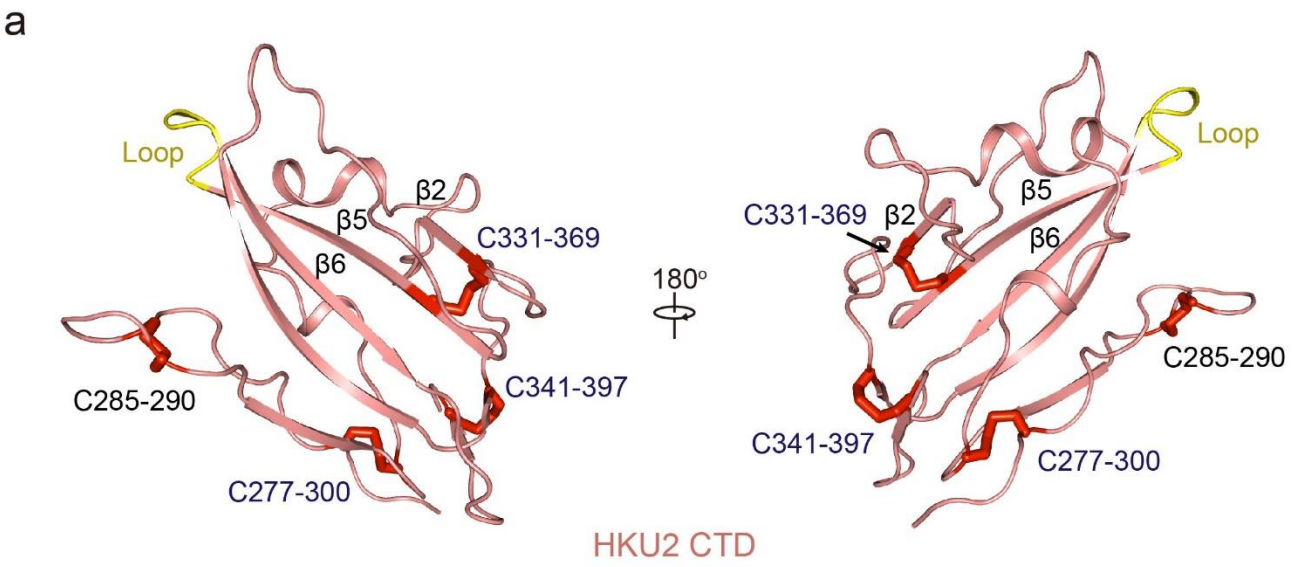

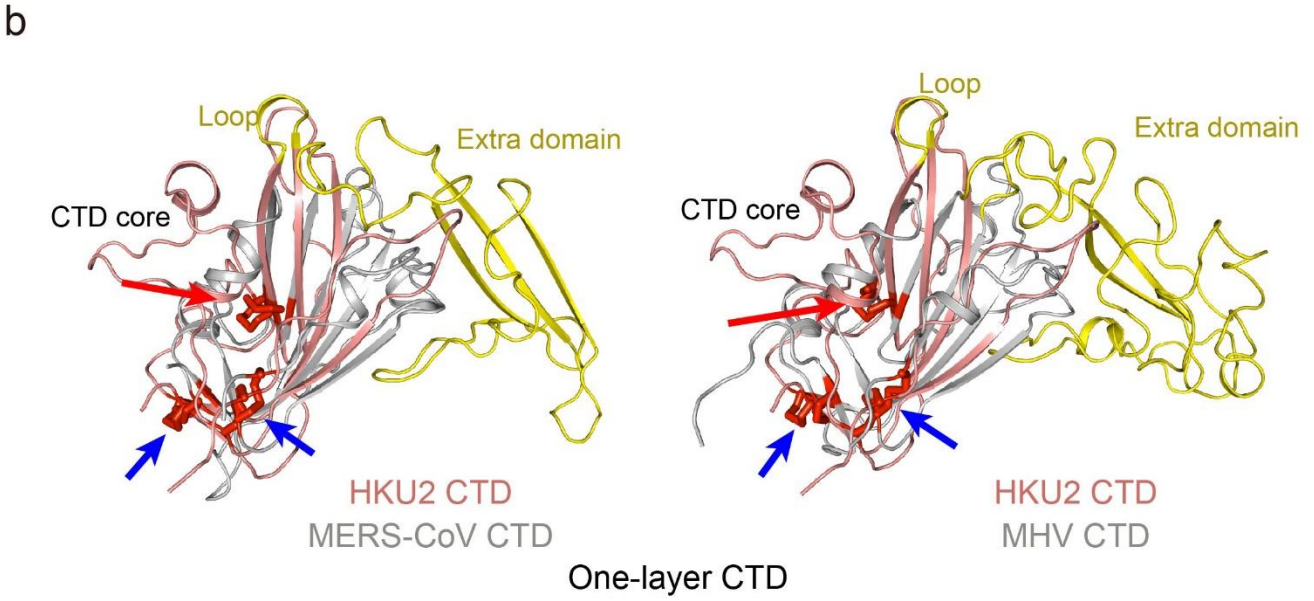

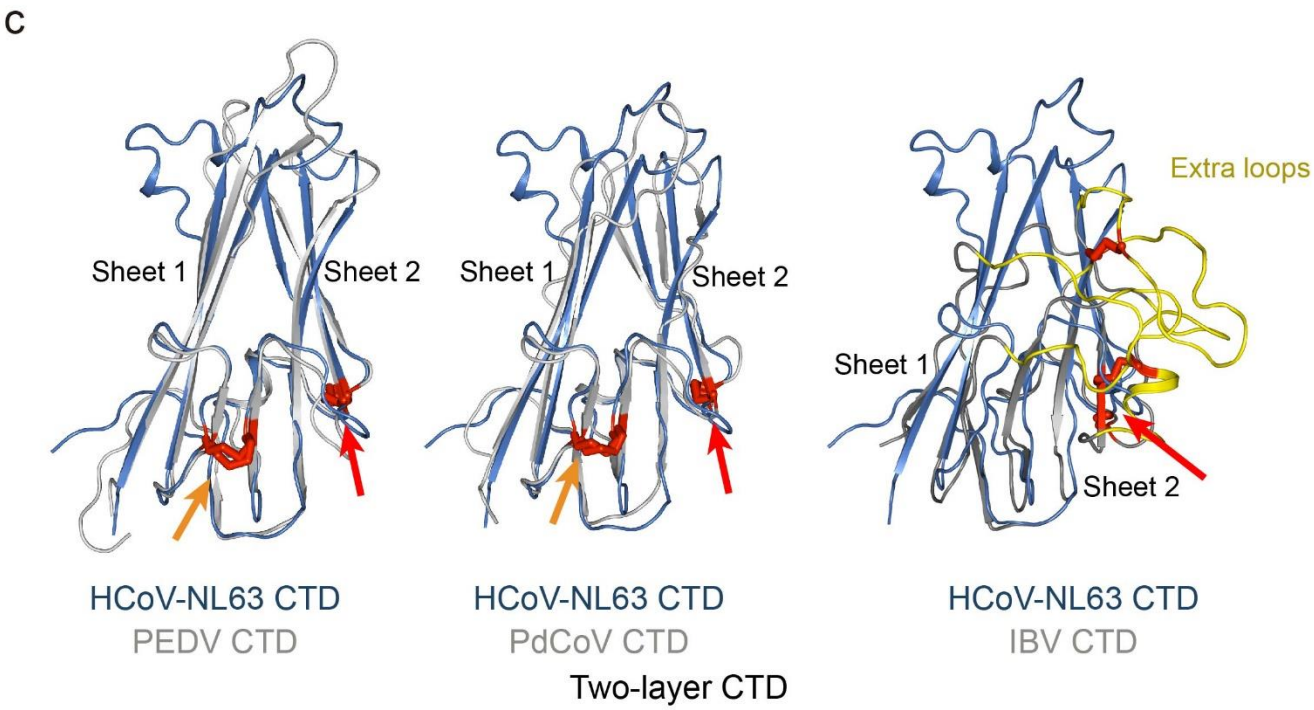

Fig. 3 Structure of HKU2 CTD and comparisons. (a) HKU2 CTD shown in two opposite directions. Strands mentioned in the main text are labeled. The loop replaced by extra domain in β-coronavirus CTDs is shown yellow. Disulfide bonds are shown as red sticks. Conserved disulfide bonds are labeled blue; other disulfide bonds are labeled black. **(b)** β-coronavirus CTDs belong to one-layer CTD. Structural alignments of HKU2 CTD with MERS-CoV CTD, and with MHV CTD are shown. Extra domains in β-coronavirus CTDs are colored yellow. Disulfide bonds are shown as red sticks. Disulfide bonds conserved in both one-layer CTD and two-layer CTD are indicated by red arrows. Disulfide bonds only conserved in one-layer CTD are indicated by blue arrows. PDB codes: MHV, 3JCL; MERS-CoV, 6Q05. **(c)** α-coronavirus (except HKU2 and SADS), γ-coronavirus, and δ-coronavirus CTDs belong to two-layer CTD. Structural alignments of HCoV-NL63 CTD with PEDV CTD, with PdCoV CTD, and with IBV CTD are shown. Two layers of β sheets are labeled. Extra loops in IBV CTD are colored yellow. Disulfide bonds are shown as red sticks. Disulfide bonds conserved in both one-layer CTD and two-layer CTD are indicated by red arrows. Disulfide bonds only conserved in two-layer CTD are indicated by orange arrows. PDB codes: HCoV-NL63, 5SZS; PEDV, 6U7K; IBV, 6CV0; PdCoV, 6B7N.

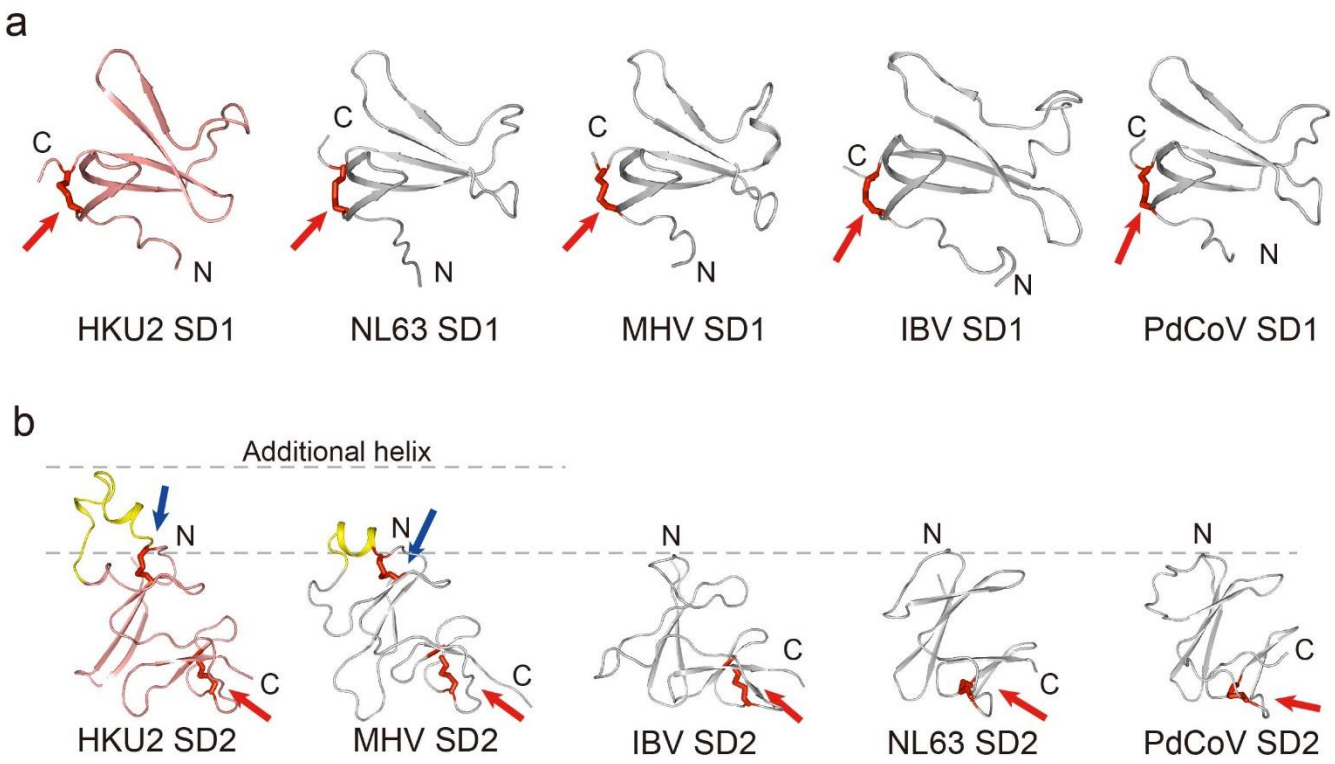

Fig. 4 Structures of SD1 and SD2 and comparisons. (a) Comparison of SD1 from four genera of coronaviruses. HKU2 SD1 is colored salmon; SD1 from other coronaviruses are colored gray. Disulfide bonds are shown as red stick. Red arrows indicate the disulfide bonds conserved in all genera of coronaviruses. PDB codes: HCoV-NL63, 5SZS; MHV, 3JCL; IBV, 6CV0; PdCoV, 6B7N. **(b)** Comparison of SD2 from four genera of coronaviruses. HKU2 SD2 is colored salmon; SD2 from other coronaviruses are colored gray. Disulfide bonds are shown as red stick. Red arrows indicate the disulfide bonds conserved in all genera of coronaviruses. Blue arrows indicate the disulfide bonds only found in HKU2 (and SADS-CoV) and βCoVs. The additional helices of SD2 from HKU2 (and SADS-CoV) and βCoVs are colored yellow and partitioned by gray dashed lines. PDB codes: HCoV-NL63, 5SZS; MHV, 3JCL; IBV, 6CV0; PdCoV, 6B7N.

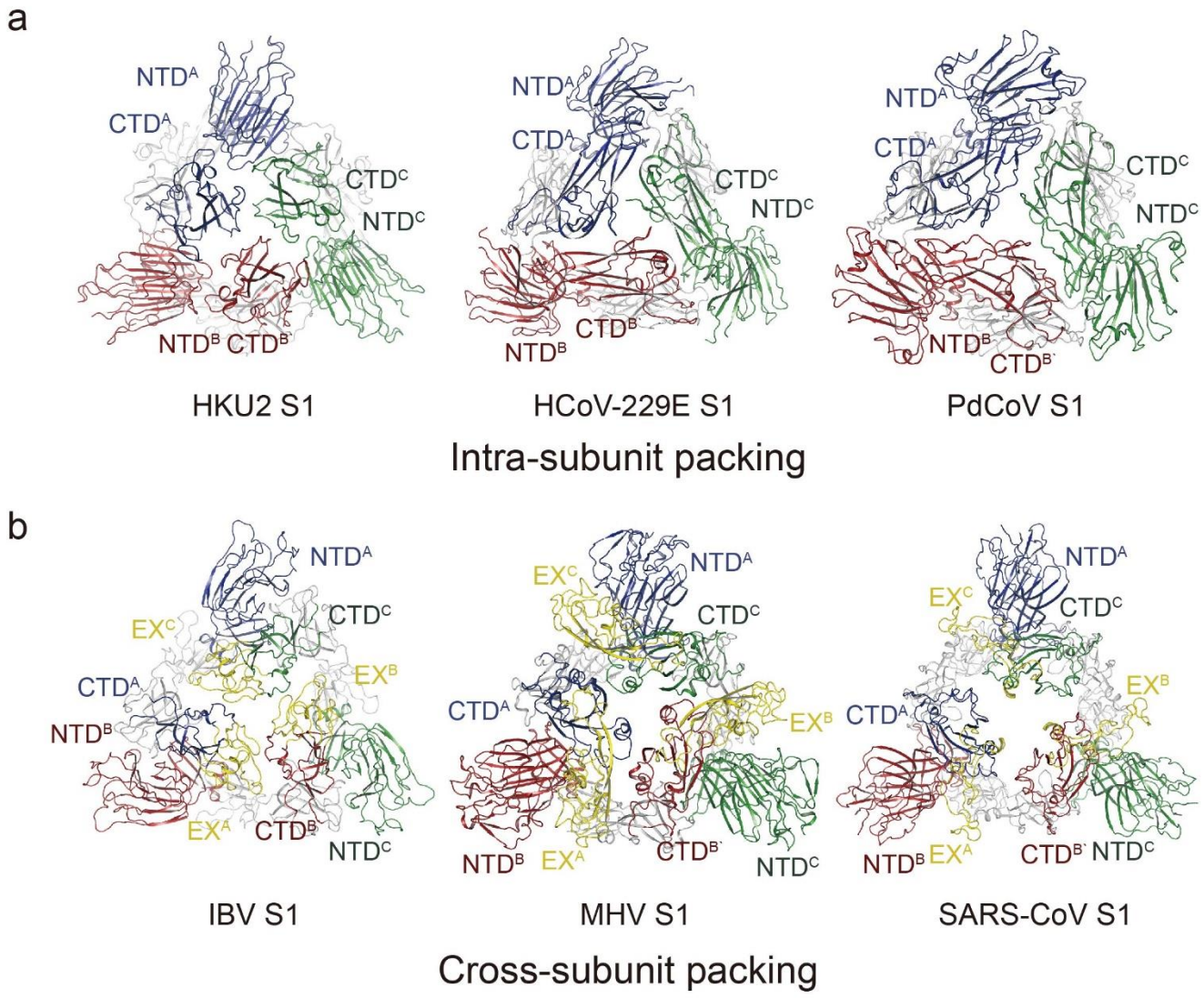

Fig. 5 Quaternary packing of NTD and CTD. (a) α-coronavirus S1 and δ-coronavirus S1 use intra-subunit packing pattern. NTD and CTD from the first monomer are colored blue, the second are colored red, and the third are colored green. PDB codes: HCoV-229E, 6U7H; PdCoV, 6B7N. **(b)** β-coronavirus S1 and γ-coronavirus S1 use cross-subunit packing pattern. NTD and CTD from the first monomer are colored blue, the second are colored red, and the third are colored green. The extra loop of IBV and the extra domains of βCoVs are colored yellow and labeled as EX. PDB codes: MHV, 3JCL; IBV, 6CV0; SARS, 5XLR.

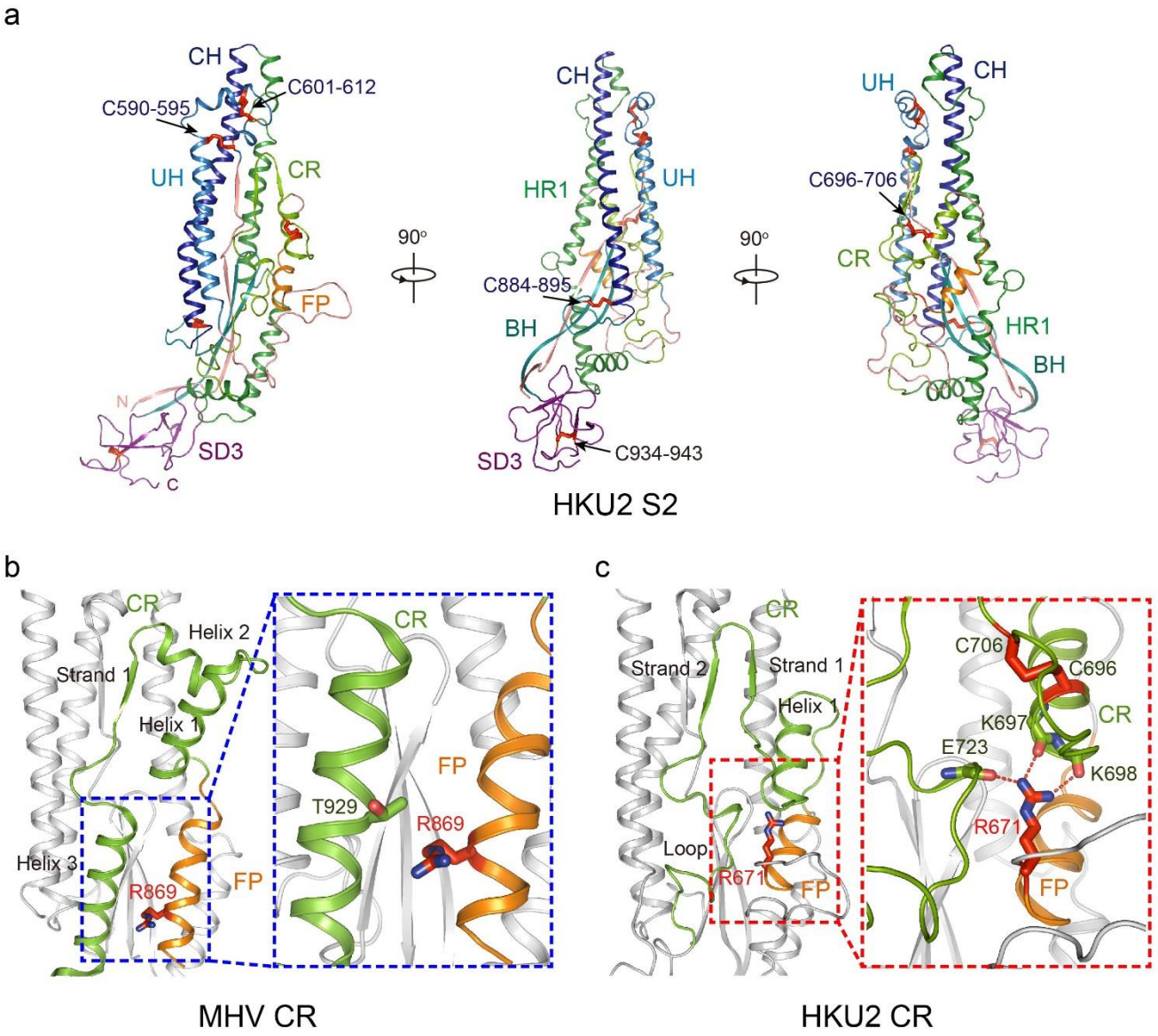

Fig. 6 Structure of HKU2 S2. (a) Side views of HKU2 S2 shown in three directions. Seven segments of S2 are shown as different colors. UH, upstream helix; FP, fusion peptide; CR, connecting region; HR1, heptad repeat 1; CH, central helix; BH, β-hairpin; SD3, subdomain 3. Disulfide bonds are shown as red stick. Disulfide bonds conserved in all coronaviruses are labeled blue; the other disulfide bond is labeled black. **(b)** Conserved CR represented by MHV CR. CR and FP are colored the same as in a. Helices and strands in CR are labeled. R869 (S2' cleavage site) is shown as stick and colored red. The blue dashed box shows R869 does not interact tightly with MHV CR. PDB code: MHV, 3JCL. **(c)** Unique feature of HKU2 CR. CR and FP are colored the same as in a. Helices and strands in CR are labeled. R671 (S2' cleavage site) is shown as stick and colored red. The red dashed box shows detailed interactions between R671 and CR.